Efficiency Enhancement in Air Heat Exchangers: Analyzing the Impact of Size Ratio and Geometric Modifications on Delta-Wing Vortex Generators

Pedro Popelka*[iD], Álvaro Valencia[iD]

Department of Mechanical Engineering, Universidad de Chile, 8370456 Santiago, Chile

* Correspondence: Pedro Popelka (pedro.popelka@ug.uchile.cl)

Citation: P. Popelka and A. Valencia, "Efficiency enhancement in air heat exchangers: Analyzing the impact of size ratio and geometric modifications on delta-wing vortex generators," *Power Eng. Eng. Thermophys.*, vol. 2, no. 4, pp. 212–227, 2023. https://doi.org/10.56578/peet020403.

Abstract: In the domain of compact flat plate heat exchangers, enhancing efficiency remains a pivotal challenge, primarily due to the low thermal conductivity characteristic of the gas phase. This investigation explores efficiency improvements in such exchangers by the integration of modified delta-wing longitudinal vortex generators (LVGs). The focus is centered on geometric modifications and alterations in the size ratios of the traditional delta-wing design as documented in pertinent literature. The geometric modifications include partial surface removal and elevation from the attachment surface, as well as a combination of these approaches. Concurrently, size ratio alterations involve a systematic reduction in the overall dimensions of the modified LVGs to 75%, 50%, and 25% of their initial size. Employing ANSYS Fluent, the study conducts numerical simulations to evaluate air flow at various Reynolds numbers (Re = 2,000 – 10,000). Analyses include examining temperature progression along the axial distance, mapping temperature contours, and applying the Q-criterion for in-depth understanding. Performance evaluation of each modification was undertaken by calculating the thermal enhancement factor (TEF) in relation to a baseline scenario of two unmodified flat plates, utilizing the Nusselt number and the friction factor for comprehensive comparison. To ensure reliability, the study demonstrates mesh independence in results and validates the computational model through comparative analysis with established correlations and experimental data from existing literature on delta-wing LVG designs. Findings indicate that geometric modifications of vortex generators, as explored in this research, do not markedly decrease head loss nor significantly enhance system performance. In contrast, size ratio modifications, particularly the reduction of vortex generator dimensions to 75 % and 50 % of the original size, show an increase in TEF ranging from 3% to 9% compared to the conventional delta-wing design. This underscores the potential of incorporating an array of such modified LVGs on each plate of a flat plate heat exchanger to boost its efficiency significantly.

Keywords: Vortex generators; Heat exchangers; Turbulent flow; Delta wing; Geometric modification; Size ratio; Thermal enhancement; Computational fluid dynamics (CFD)

1 Introduction

Heat exchangers, integral in a multitude of systems such as heating and cooling, electrical power generation, petroleum refining, chemical and pharmaceutical processes, paper production, transportation industries, and many others [1], facilitate the transfer of thermal energy between two media. Air, being an abundant resource, is prevalently employed as a cooling fluid in these systems. However, its relatively low thermal conductivity, compared to fluids like water, compromises the efficiency of these devices, necessitating a significant resource allocation to achieve desired heat transfer rates. Enhancements in the gaseous phase of these systems, therefore, present substantial benefits in terms of equipment size reduction, cost savings, or operating at lower mass flow rates to maintain the same heat transfer levels. Even marginal improvements in these large-scale systems can cumulatively lead to significant resource utilization impacts. In this context, a notable study in 2023 by Agarwal [2] explored methods to augment the heat absorption performance of fluids in thermal storage systems, crucial in solar thermal power plants, achieving a considerable enhancement of 1.3% in thermal capacity.

It has been established that heat transfer rates in heat exchangers escalate in the presence of turbulent external flow [3]. Consequently, there is a growing interest in investigating methods to induce turbulence between parallel plates to bolster heat transfer. This can be achieved using LVGs, which passively induce turbulence in the flow. However, the introduction of these elements into the system accompanies an increase in head loss [3], necessitating a balanced consideration of both the induced turbulence and the resultant head loss to ascertain their overall benefit.

Within the realm of LVGs, delta-wings and delta-winglets have garnered significant attention in literature. Their ease of integration into plate walls, through simple punching methods, and their efficacy in generating vortical structures, render them particularly noteworthy in the study of heat exchanger efficiency enhancement.

1.1 Studies on LVG Angle of Attack

The impact of angle of attack on the efficiency of delta-winglet-shaped LVGs was first examined experimentally by Tiggelbeck et al. [4] in 1993. This study explored the performance of even rows of these LVGs across Reynolds number regimes from 2,000 to 8,000, both in aligned and alternating configurations. It was discovered that aligned arrangements exhibited marginally superior heat transfer performance, an optimum angle of attack 45° was associated with improved efficiency, and generally, the ratio between the Nusselt value and the C_f value increased with Re, indicating a rise in the Nusselt number and a decrease in C_f along with an increase in turbulence.

Furthering this research, Tiggelbeck et al. [5] in 1994, conducted experimental studies on various LVG types, delta wing, rectangular wing, delta winglet pair, and rectangular winglet pair, altering the angle of attack across Reynolds number regimes between 2,000 and 9,000. It was concluded that each LVG type has an angle of attack where heat transfer is maximized. By calculating the thermal enhancement factor (TEF) for Re = 4,600 for these configurations, it was inferred that all LVGs exhibited similar performance levels, except for the rectangular wing, which showed lower efficacy.

1.2 Exploration of LVG Positioning and Shape Modification

Zhou and Feng [6], in 2012, conducted experimental research on the effects of removing a portion from the surface of six varied LVG shapes under laminar and turbulent regimes (Re = 650 - 21,000). It was observed that such removals not only reduce pressure drops caused by the LVGs but also lower the system's f. However, this reduction in f was accompanied by a decrease in Nu, highlighting the necessity to maintain a balance between material removal and insertion efficiency. The position of the removal was found to have minimal impact on key system variables, leading to the conclusion that surface removal can enhance the overall system performance.

In 2016, Oneissi et al. [7] undertook computational simulations in ANSYS Fluent to investigate the effects of altering the orientation of delta winglets, originally studied by Tiggelbeck et al. [5] in 1994, across laminar to turbulent flow regimes (Re = 270-21,600). The study claimed mesh independence at a percentage difference of 1.17% to the previous Nusselt number calculation. The model exhibited deviations of 4.69, 2.09 and 4.14% in Nu, f, and TEF from the 1993 Tiggelbeck winglet pair results, demonstrating a potential for geometry optimization to reduce the friction factor of the system by up to 50%, thereby increasing TEF by 6%, attributed to a more aerodynamically efficient configuration.

Furthermore, Wijayanta et al. [8], in 2018, experimentally examined the inclusion of delta-wing shaped LVGs in a twin-tube radial exchanger using water under turbulent regimes (Re = 5,300-14,500). They varied the ratio of the LVG's wet length to the channel section, finding that both Nu, f and TEF performance improved with increasing length ratio. The highest ratio of 0.63 yielded a considerable thermal improvement of 177%, an increase in friction of 11.6 times, and the best TEF performance, measured at 1.15.

In 2019, Garelli et al. [9] utilized ANSYS Fluent to simulate the effects of including delta-wing shaped LVGs in flat plate exchangers for electric transformer radiators, studying variables such as the angle of attack and the separation distance from the wall. This research, modeling the phenomenon as a natural convection problem across a spectrum of flow regimes (Re = 1,519-5,316), concluded that elevating the LVG from the wall surface optimizes the TEF performance, with an ideal value of 3 mm, and an optimal angle of attack of 30° delivering the best TEF performance of about 1.09.

Summarizing, research by Zhou and Feng [6], Oneissi et al. [7], Wijayanta et al. [8], and Garelli et al. [9] indicates that shape and size modifications of LVGs can significantly influence system performance. Specifically, Zhou and Feng [6] reported reduced friction losses through surface removal in winglet-shaped LVGs, while Garelli et al. [9] observed similar friction reduction by lifting delta-wing-shaped LVGs in natural convection systems. These findings inspire the integration of such modifications in delta-wing-shaped LVGs across varying turbulence regimes.

Throughout the years, a diverse range of LVGs has been proposed by various researchers, each characterized by unique spatial configurations and demonstrating a spectrum of performance levels. This study aims to explore the effects of geometric modifications and size ratio changes on the performance of delta-wing LVGs in air heat exchangers. Utilizing the traditional delta wing design proposed by Tiggelbeck et al. [5], this research will undertake modifications including surface removal, lifting relative to the wall, and their combination. Additionally, the study

will evaluate the impact of progressively reducing the size of a modified LVG, maintaining a constant channel section. The goal is to achieve a more significant reduction in head loss than in heat transfer, thereby enhancing the overall performance of the delta wing LVG and, consequently, the efficiency of the system.

2 Methodology

The methodology of this study is underpinned by a numerical modeling approach, utilizing computational fluid dynamics (CFD) to simulate the targeted phenomena. The computational domain encompasses a smooth channel and a delta-wing, including variations in its geometry and size ratio. This methodology is grounded in the application of fundamental fluid dynamics equations, coupled with a turbulence model, effectively creating a virtual laboratory environment for detailed exploration. This approach facilitates a rigorous examination of key parameters, thereby enriching the understanding of fluid dynamics and heat transfer behaviors in the context of the study.

2.1 Numerical Model

For the simulation of physical phenomena in various study cases, a three-dimensional Reynolds-Averaged Navier-Stokes (RANS) Standard $\kappa - \omega$ steady-state model was employed, utilizing ANSYS Fluent 18.2. In these simulations, air, serving as the working fluid, was considered a Newtonian and incompressible fluid. The software employs a cell-centered finite element discretization method to solve the conservation equations for mass, momentum, and energy. This approach utilizes a turbulence simplification, decomposing the flow into mean and fluctuant components, thereby optimizing computational efficiency. The governing equations of the model are as follows:

Continuity equation:

$$\frac{\partial}{\partial x_i}\left(\rho u_i\right) = 0 \tag{1}$$

Momentum equation:

$$\frac{\partial}{\partial t}\left(\rho u_i\right) + \frac{\partial}{\partial x_j}\left(\rho u_i u_j\right) = -\frac{\partial p}{\partial x_i} + \frac{\partial}{\partial x_j}\left[\mu\left(\frac{\partial u_i}{\partial x_i} + \frac{\partial u_j}{\partial x_i} - \frac{2}{3}\delta_{ij}\frac{\partial u_1}{\partial x_i}\right)\right] + \frac{\partial}{\partial x_i}\left(-\rho\overline{u'_l u'_j}\right) \tag{2}$$

Energy equation:

$$\frac{\partial}{\partial x_i}\left(\rho u_i C_p T\right) = \frac{\partial}{\partial x_i}\left(k_{eff}\frac{\partial T}{\partial x_i}\right) \tag{3}$$

In these equations, ρ represents density $\left(\mathrm{kg/m^3}\right)$, u velocity $(\mathrm{m/s})$, t time (s), p pressure (Pa), μ dynamic viscosity $(\mathrm{kg/m \cdot s})$, C_p specific heat $(\mathrm{J/kg \cdot K})$, k_{eff} effective thermal conductivity $(\mathrm{W/m \cdot K})$, and T temperature (K).

The Standard $\kappa - \omega$ model's transport equations are delineated as:

$$\frac{\partial}{\partial t}(\rho\kappa) + \frac{\partial}{\partial x_i}\left(\rho\kappa u_i\right) = \frac{\partial}{\partial x_j}\left(\Gamma_\kappa\frac{\partial\kappa}{\partial x_j}\right) + G_\kappa - Y_\kappa + S_\kappa + G_b \tag{4}$$

$$\frac{\partial}{\partial t}(\rho\omega) + \frac{\partial}{\partial x_i}\left(\rho\omega u_i\right) = \frac{\partial}{\partial x_j}\left(\Gamma_\omega\frac{\partial\omega}{\partial x_j}\right) + G_\omega - Y_\omega + S_\omega + G_{\omega\mathrm{b}} \tag{5}$$

where, κ signifies turbulent kinetic energy, and ω the specific dissipation rate. G_κ denotes the generation of turbulent kinetic energy due to mean velocity gradients, whereas G_ω represents the generation of ω. Γ_κ and Γ_ω are the effective diffusivity terms for κ and ω, respectively, and Y_κ and Y_ω denote the dissipation of these energies due to turbulence. S_κ and S_ω are user-defined source terms, G_b and $G_{\omega\mathrm{b}}$ and incorporate buoyancy effects. Further details on the model can be found in the ANSYS Fluent Theory Guide [10].

The modeling approach included the use of a SIMPLEC pressure-based solver, absolute velocity formulation, a 5 % turbulence intensity at the inlet, and a skewness correction of 0. Gradient discretization was handled through a least squares method, with second-order discretization for pressure, energy, turbulent kinetic energy, and momentum, and first-order discretization for the specific dissipation rate. Convergence of the solution was defined by residual values of 10^{-4} for continuity, and 10^{-6} for velocities, κ and ω.

2.2 Computational Domain

The replication of an entire heat exchanger, comprising numerous flat plates, in a computational model would necessitate prohibitively high computational resources. Recognizing the inherent symmetry and periodicity in these systems, the problem formulation was simplified to a basic replicable unit (Figure 1), as facilitated by tools in the modeling software. This approach allows for the extrapolation of the behavior of the entire system from the results obtained for the basic unit. The defined control volume corresponds to the space occupied by the fluid within it.
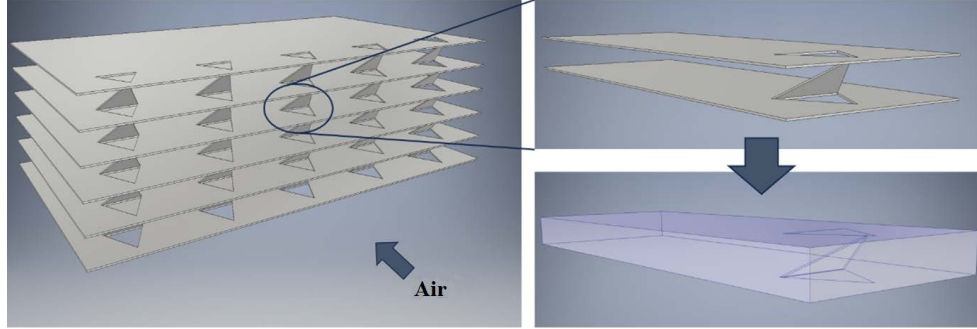
Figure 1. Simplification of the problem and formulation of the control volume

For an accurate representation of the real-world scenario, boundary conditions were meticulously selected (Figure 2). Drawing on experimental setups from existing literature, the following conditions were established: a uniform air inlet at a constant temperature T_{in}= 20℃ and velocity u_{in}= 0.804; 1.608; 2.412; 3.216; 4.021, a pressure outlet, symmetry conditions on the two longer sides of the domain, an adiabatic condition on the LVG, constant wall temperatures T_w above and below 50℃, and periodicity conditions at the punching holes. The fluid properties were evaluated at a mean temperature T_m, corresponding to ρ=1.164 (kg/m^3), $\mu = 1.872 \cdot 10^{-5}$ (kg/m · s), C_p=1,007 (J/kg · K), k=2.588 · 10^{-2} (W/m · K) and Pr=7.284 · 10^{-1}.
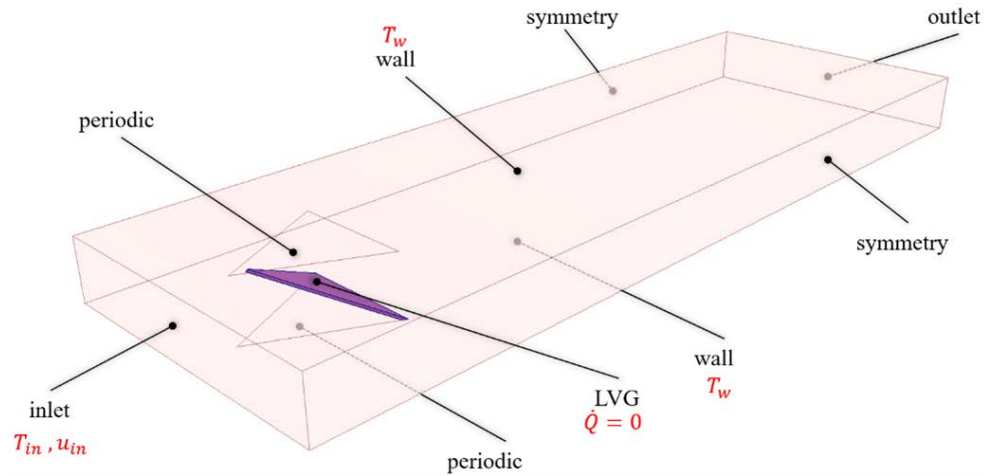
Figure 2. Boundary conditions of the model, with imposed magnitudes marked in red

The study involved examining geometric modifications of the delta wing, as per the 1994 study by Tiggelbeck et al. [5] (Figure 3), and size-ratio modifications of a geometrically modified LVG (Figure 4). In the scope of geometric modifications, the LVG was first elevated by 2.5 mm from the wall ($DW(L)$), aiming to replicate results akin to the 2019 study by Garelli et al. [9]. Then 20% of its original surface area was removed, targeting outcomes observed in the 2014 study by Zhou and Feng [6] ($DW(R)$). Lastly, the combined effects of both modifications were explored ($DW(R+L)$). For size-ratio modifications, all dimensions of the modified $DW(R+L)$ LVG were reduced to 75%, 50%, and 25% of their initial dimensions, maintaining a constant channel section. These cases were designated as $DW(R+L)(0.75)$, $DW(R+L)(0.50)$, and $DW(R+L)(0.25)$.

The modeling dimensions for each study case are summarized in Table 1. The performance of each LVG configuration was evaluated against a base case, comprising a plain channel formed by two parallel plates of specific dimensions $H \times B \times L$.
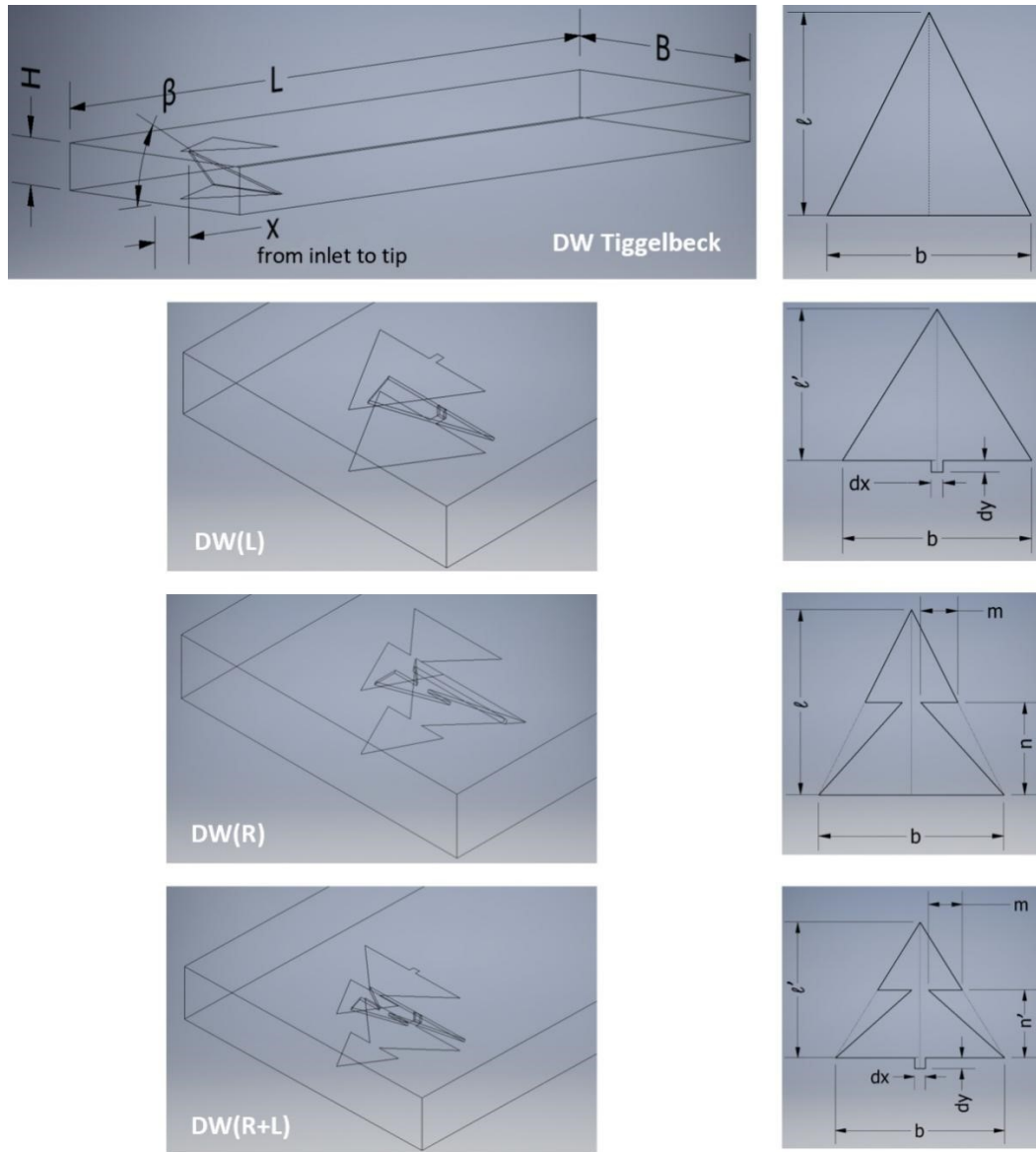
Figure 3. Original delta-wing and geometric modification study cases

Figure 4. Front view of the original $DW(R+L)$ and size-ratio modification study cases

Table 1. Model dimensions (mm)

Channel			LVGs									
H	B	L	x	β	b	l	l'	m	n	n'	dx	dy
20	$5H = 100$	$15H = 300$	20	30	40	40	32	8	20	16	2.5	2.5

2.3 Calculation of Quantities

In the context of heat exchangers, heat transfer predominantly occurs through convection, supplemented by conduction and radiation. This study concentrates on enhancing the convective heat transfer rate, as it is the primary mechanism in such systems. The convective heat flux, central to this analysis, is defined in accordance with the methodology of Tiggelbeck et al. [5]:

$$\dot{Q} = \bar{h} A \left(T_w - T_{in} \right) \tag{6}$$

where, $\dot{Q}(W)$ represents the convective heat flux, $\bar{h} \left(W/m^2 \cdot K \right)$ is the mean convective heat transfer coefficient, $A \left(m^2 \right)$ denotes the wall surface, and $T_w(K)$ and $T_{in}(K)$ are the temperatures of the wall and the fluid's bulk at the channel entrance, respectively. The thermal performance of the systems is quantified using the average Nusselt number [7]:

$$\overline{Nu} = \frac{D_h \cdot \bar{h}}{k} \tag{7}$$

where, k (W/m $\cdot$ K) is the thermal conductivity of the fluid, and $D_h(m)$ is the hydraulic diameter of the channel, computed as [11]:

$$D_h = \frac{4A_t}{P_w} = 2H \tag{8}$$

where, $A_t \left(m^2 \right)$ represents the cross-sectional area of the channel, $P_w(m)$ is the wetted perimeter, and $H(m)$ is the channel height. The fluid's physical properties are evaluated at a mean temperature $T_m = \left(T_{in} + T_w \right) /2$. The simulations spanned a range of turbulence degrees, from transitional to fully turbulent regimes (Re=2,000; 4,000; 6,000; 8,000; 10,000), paralleling the approach of Tiggelbeck et al. [4, 5]. The fluid's entrance velocity u_{in} (m/s) was determined using the Reynolds number definition [12]:

$$Re = \frac{\rho u_{in} D_h}{\mu} \tag{9}$$

The fluid velocity, channel geometry with LVG insertion, and surface roughness significantly impact the system's head loss due to skin friction. This effect is quantified using the Darcy-Weisbach friction coefficient [11]:

$$f = \frac{2\Delta p}{\rho u_{in}^2} \frac{D_h}{L} \tag{10}$$

where, $\Delta p(Pa)$ signifies the total pressure loss between the inlet and outlet, and $L(m)$ is the total length of the channel. Given that LVG addition affects both Nu and f, an equivalent comparison across different cases necessitates TEF, which evaluates the increase in heat transfer and friction loss compared to a base case. This factor enables the assessment of the thermal performance of various systems under identical pumping power conditions [8]:

$$TEF = \left. \frac{h}{h_0} \right|_{pp} = \left. \frac{Nu}{Nu_0} \right|_{pp} = \frac{Nu}{Nu_0} \left(\frac{f}{f_0} \right)^{1/3} \tag{11}$$

where, Nu and f pertain to the case with LVG insertion, while Nu_0 and f_0 refer to the base case, represented in this study by an empty, smooth channel. A system exhibiting a TEF value less than 1 indicates a detrimental effect on efficiency, a value equal to 1 implies no improvement over the base case, and a value greater than 1 signifies an enhancement in the efficiency of the plain channel.

3 Results

In this study, the Nusselt number values were determined using Eqs. (6) and (7), based on the simulated heat flux values at the lower wall of the system and its surface A, aligning with the approach used in Tiggelbeck et al. [5] experiment. The friction factor f was calculated using Equation 10 from the simulated total pressure of the system ($p_{dyn} + p_{st}$).

In the experimental research of Tiggelbeck et al. [5], system friction was evaluated by calculating the drag force F_d (Eq. (12)), which was then normalized by the cross-sectional area A_t, yielding the drag coefficient C_f, equivalent to $f/4$. For consistency with these results, pressure values in this study's simulations were obtained through an area-weighted average for the model validation case under Re=4,600. For other scenarios, the values were derived from a mass-weighted average to reflect the dynamic pressure based on fluid velocity.

$$C_f = \frac{2F_d}{\rho u_{in}^2 A_t} \tag{12}$$

3.1 Mesh Independence

Mesh independence was assessed under the highest turbulence degree Re = 10,000 by analyzing the variations in simulated values of Nu and f across different mesh refinement levels. The process commenced with a coarse mesh, progressively enhancing wall refinement and reducing the size of the first inflation layer (Table 2). At the fourth level of refinement, the model utilized 901 thousand elements with a first cell size of 0.1 mm, yielding an average skewness quality of 0.22 and a maximum value of 0.66. This refinement level produced a maximum value of y^+ of 0.83, resulting in a percentage decrease of 0.6% and 0.2% in Nu and f values, respectively. These reductions align with the 1.17% criterion established by Oneissi et al. [7], affirming the convergence and mesh independence of the results.

Table 2. Mesh sensibility analysis

Mesh	Element Quantity (thousands)	Max Element Size (mm)	Max Face Size (mm)	Inflation Size (mm) - Layers	%Nu	%f
1	325	2.0	2.0	$0.3 - 5$		
2	355	2.0	2.0	$0.2 - 5$	-6.9	-7.2
3	528	2.0	1.7	$0.1 - 5$	-4.8	-4.8
4	901	2.0	1.3	$0.1 - 5$	-0.6	-0.2

3.2 Numerical Validation

3.2.1 Base case

The simulation results for the plain channel were compared with established correlations in the literature applicable to fully turbulent regimes. For the Nusselt number, the Dittus-Boelter correlation portrayed in study [13] was utilized (Eq. (13)), while the Petukhov correlation used in research [14] was applied for the friction coefficient (Eq. (14)). Table 3 presents the percentage differences between the simulations and these correlations.

$$Nu = 0.023 Re^{0.8} \Pr^{0.4} \tag{13}$$

$$f = (1.82 \log_{10} Re - 1.64)^{-2} \tag{14}$$

**Table 3.** Percentage difference between simulated values and correlations for the plain channel

Re	Nu Dittus-Boelter	f Petukhov
2,000	40%	40%
4,000	18%	16%
6,000	10%	8%
8,000	6%	5%
10,000	4%	3%

It was observed that the alignment of Nu and f with the correlations improved as the Reynolds number increased (Figure 5), while higher errors were noted in lower flow regimes. The deviations can be attributed to two factors: firstly, the correlations are designed for fully turbulent regimes $Re > \sim 4000$, and secondly, the differences in the inlet boundary condition. The simulations assumed a uniform velocity condition at the inlet (subgraphs (a) and (b) of Figure 6), which deviates slightly from real scenarios where a non-uniform velocity profile typically develops. However, a distinct velocity profile was observed immediately downstream of the inlet (subgraphs (c) and d) of

Figure 6). At Re=2,000, the velocity profile differed significantly from the uniform condition, whereas at higher turbulence degrees, the profile more closely resembled the uniform shape. This accounts for the progressively decreasing error between the simulated results and the correlations as the turbulence degree increased. Despite these discrepancies, the model was deemed valid, as the overestimation was relatively consistent for both Nu and f.
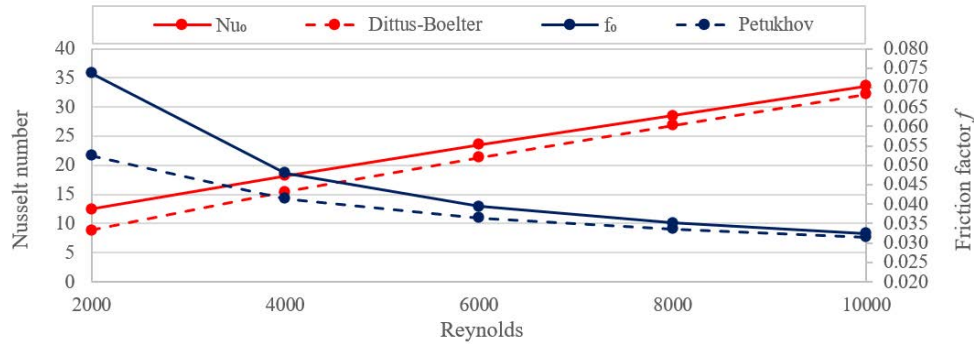
Figure 5. Comparison of simulation results with correlations for the plain channel
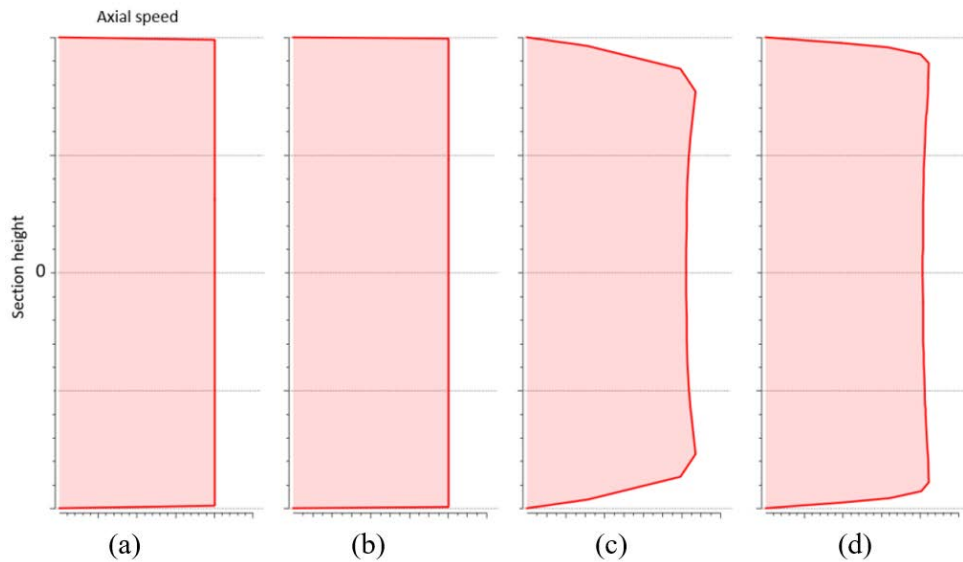
Figure 6. Axial speed profiles in the plain channel: (a) At inlet for Re=2,000; (b) At inlet for Re=10,000; (c) At 3% L downstream for Re=2,000; (d) At 3% L downstream for Re=10,000

Table 4. Validation simulation results

|	**Tiggelbeck et al. [5]**	**Simulation**	**Error**
Nu/Nu_0	1.36	1.28	-6%
f/f_0	1.50	1.54	3%
TEF	1.186	1.107	-7%

3.2.2 Model validation

The model validation involved simulating the delta-wing design from Tiggelbeck et al. [5] for a Reynolds number of 4,600 under specific boundary conditions (T_{in}= 24℃ and T_w= 30.8℃, with ρ=1.140 (kg/m^3), μ=1.901·10^{-5} (kg/m · s), C_p=1,007 (J/kg · K), k=2.635 · 10^{-2} ($W/m · K$) and Pr=7.266 · 10^{-1}. Table 4 compares these results with the experimental data from Tiggelbeck et al. [5] The computational model exhibited a -6% error in Nu/Nu_0 values, a 3% deviation in f/f_0, and a 7% underestimation in TEF compared to the experimental findings. The magnitude of errors in this study and the 2016 study by Oneissi et al. [7] were comparable, with the notable difference being the tendency of the current model to slightly underestimate the heat transfer enhancement due to LVG insertion.

Despite this, the model was validated as accurate, with the caveat that the thermal enhancement in the case studies might be marginally understated.

3.3 Geometric Modifications

In the upstream region of the insertions, it was observed that these modifications exerted negligible impact on the mean fluid temperature within the Re=6,000 regime, as depicted in Figure 7. Conversely, downstream of the insertions, a progressive deviation in the temperature trends was noted, indicative of enhanced thermal exchange compared to the base case of flat plates. The geometric alterations to the delta wing did not significantly affect the final fluid temperature, suggesting that these modifications have a minimal influence on the thermal performance of the original geometry.
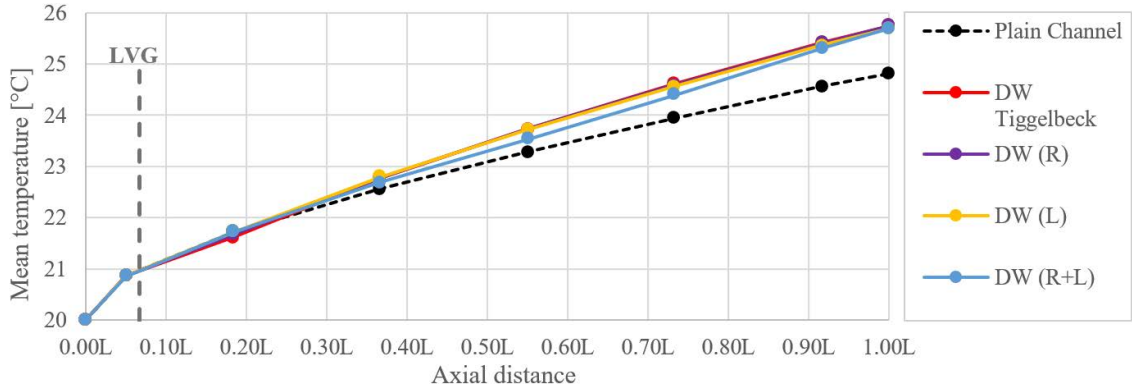
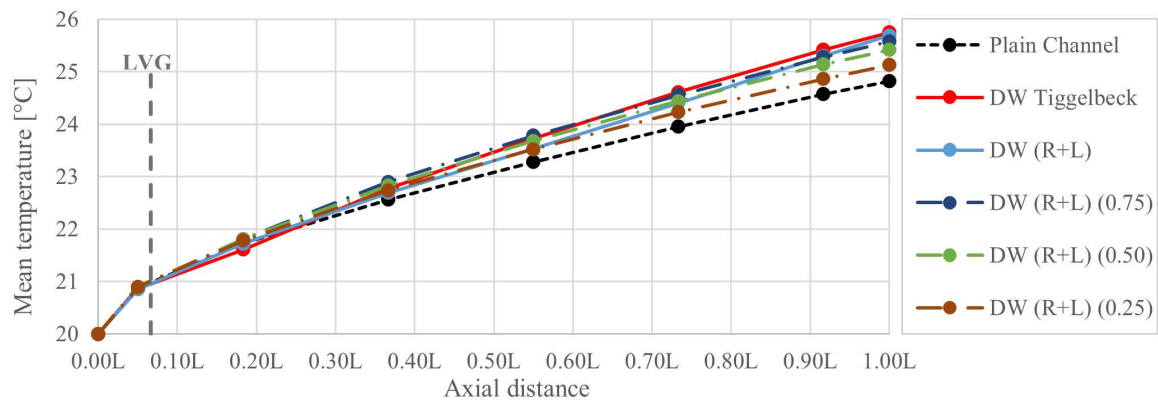**Figure 7.** Mean temperature along axial position in geometric modification study cases (Re=6,000)
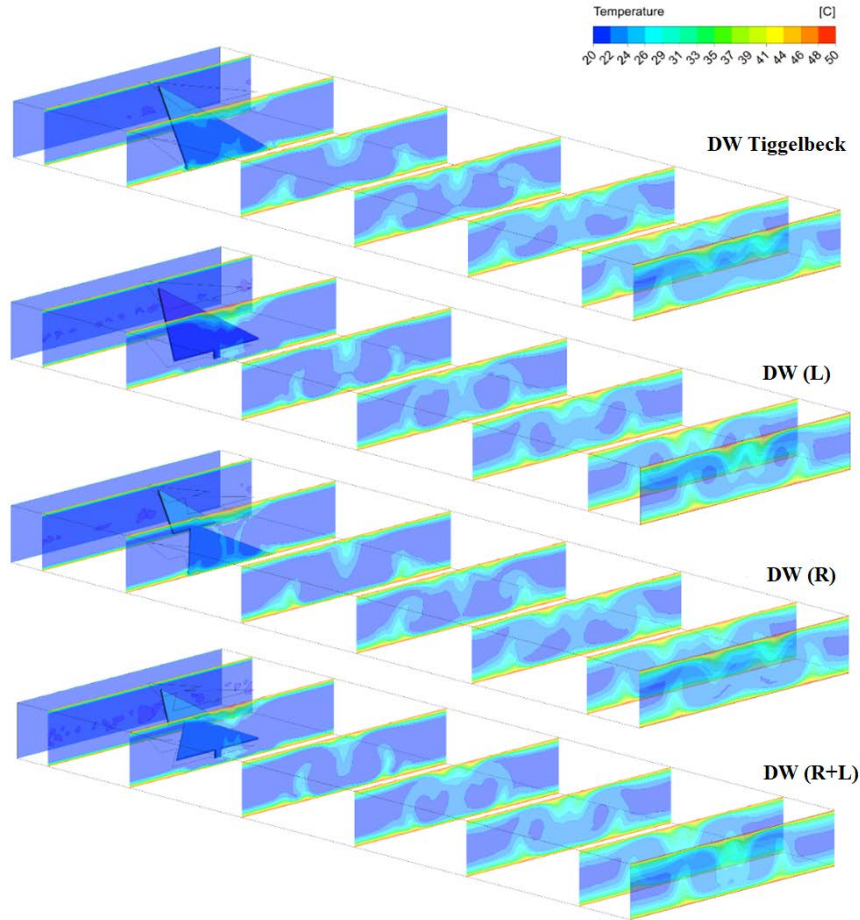
Figure 8. Temperature development in geometric modification study cases (Re=6,000)

The influence of the insertions on fluid mixing was elucidated through temperature contours along the channel at Re = 6,000 (Figure 8). The vortical structures, induced by the insertions, altered the flow trajectories, leading to enhanced fluid mixing that directly affected the thermal boundary layer of the system. In all cases, these structures facilitated the rotation of fluid segments from the walls towards the central part of the channel, ensuring continuous fluid replacement throughout the system. When comparing the traditional delta wing with the modified insertions, it was found that their influence locations were relatively similar, with no substantial divergence in impact. This is consistent with the observation that the increase in fluid temperature across all geometric modification cases was akin to the delta wing design by DW Tiggelbeck.

3.4 Size-Ratio Modifications

Similar to previous cases, the presence of insertions upstream was observed to have no effect on the mean fluid temperature, as shown in Figure 9. Post-insertion, the temperature increase demonstrated a direct correlation with the size of the LVG. It was noted that a reduction in the size of the LVG led to a decrease in the thermal performance of the system, aligning it more closely with the base case. This finding suggests that the thermal performance is significantly influenced by modifications of this nature.

**Figure 9.** Mean temperature along axial position in size-ratio modification study cases (Re=6,000)
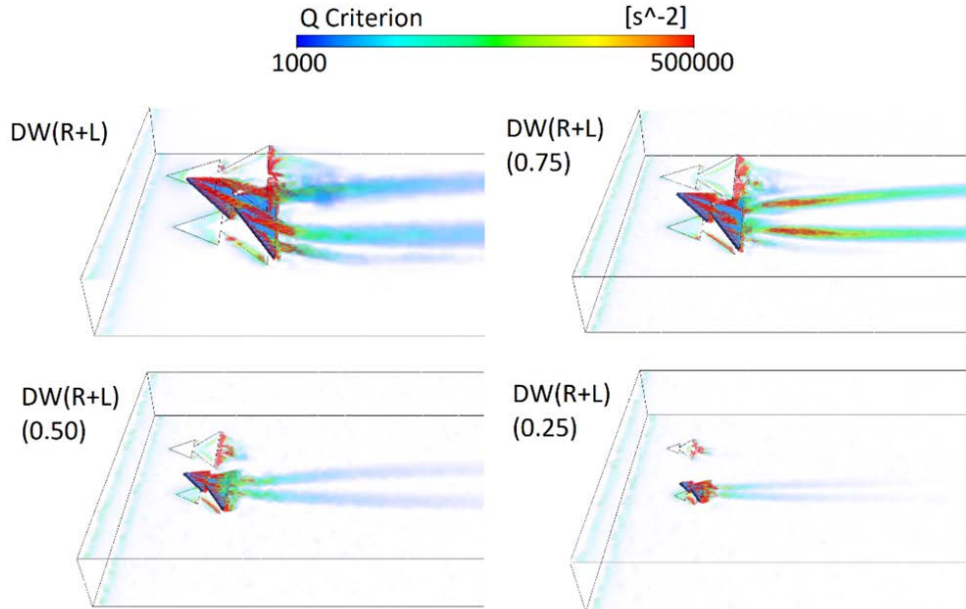
Figure 10. Visualization of vortical structures using the Q-criterion (Re=6,000)

The extent of vorticity generated in these scenarios was quantified using the Q-criterion (Eq. (15)), which identifies regions where the Euclidean norm of the vorticity tensor (Ω) surpasses that of the rate of strain (S) [15]. The results derived from this criterion, illustrated in Figure 10, indicate that a reduction in size directly diminishes

turbulence generation. The impact of the vortical structures produced by varying insert sizes on the fluid along the channel is depicted in Figure 11 via temperature contours. As hypothesized, a decrease in the magnitude of the vortical structures led to a reduced area of influence, consequently diminishing the perturbation of the thermal boundary layer and, therefore, the thermal performance.

$$Q = 0.5 \left(|\Omega|^2 - |S|^2 \right) \tag{15}$$
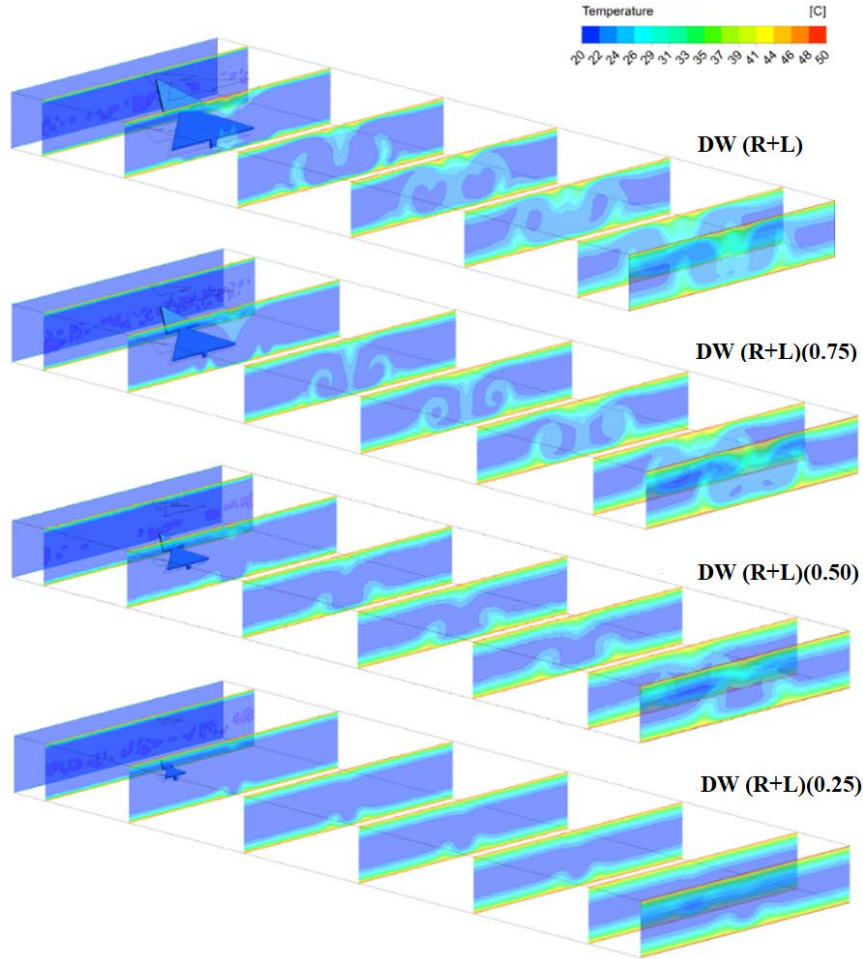
Figure 11. Temperature development in size-ratio modification study cases (Re=6,000)

3.5 Global Performance of Modified LVGs

The global performance of all study cases, in terms of the Nusselt number, friction factor, and TEF, is depicted in Figure 12, Figure 13, annd Figure 14.

In this study, modifications in size-ratio were implemented to enhance the original geometry's TEF. However, these geometric modifications did not surpass the performance benchmarks set by delta wing Tiggelbeck (DW Tiggelbeck), notable in the metrics of Nu, f and TEF. The implications of these modifications warrant further analysis. It was observed that the modifications did not alter the trend of the TEF curves but resulted in their vertical shift on the graph. Preliminary simulations indicated that DW (R) would not significantly differ from the results of DW Tiggelbeck for $Re = 6,000$, leading to the decision against further simulation at varying Reynolds numbers. A critical aspect of each case involves the examination of favored flow paths. Both surface removal and lifting modifications aim to reduce system head loss by creating new fluid pathways, with minimal impact on heat transfer efficiency. Table 5 delineates the distribution of total mass flow through the channel section and the punching hole, as depicted in Figure 15. In scenarios DW (L) involving lifting equivalent to 13% surface removal, an increased flow of 2% through the channel section was recorded, yet a considerable portion of 10% still navigated through the punching hole. This phenomenon led to a nominal decrease in system friction and culminated in the highest Nusselt loss, thus resulting in suboptimal TEF performance.
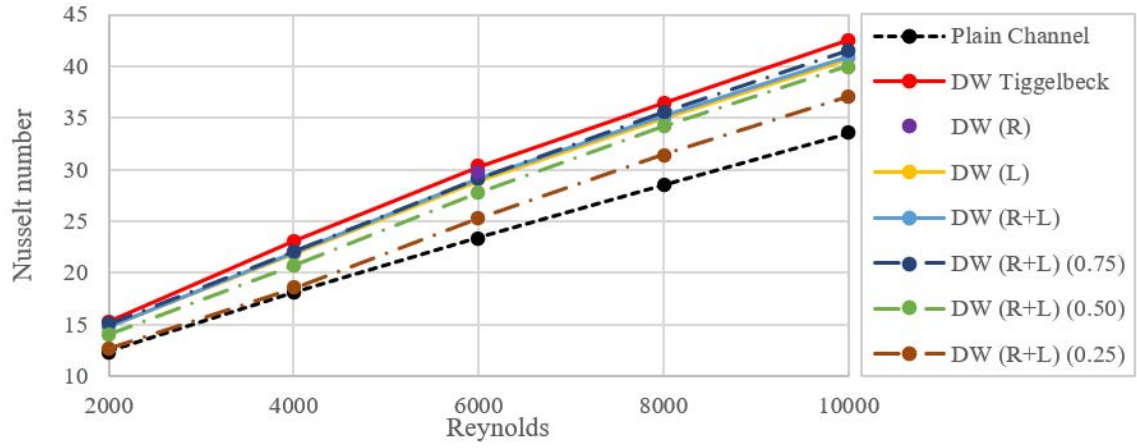
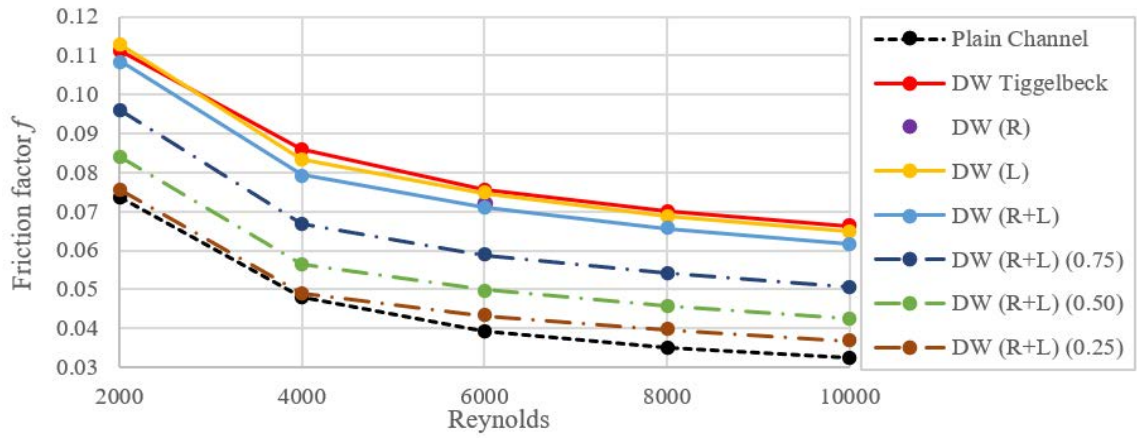**Figure 12.** Thermal performance of the study cases

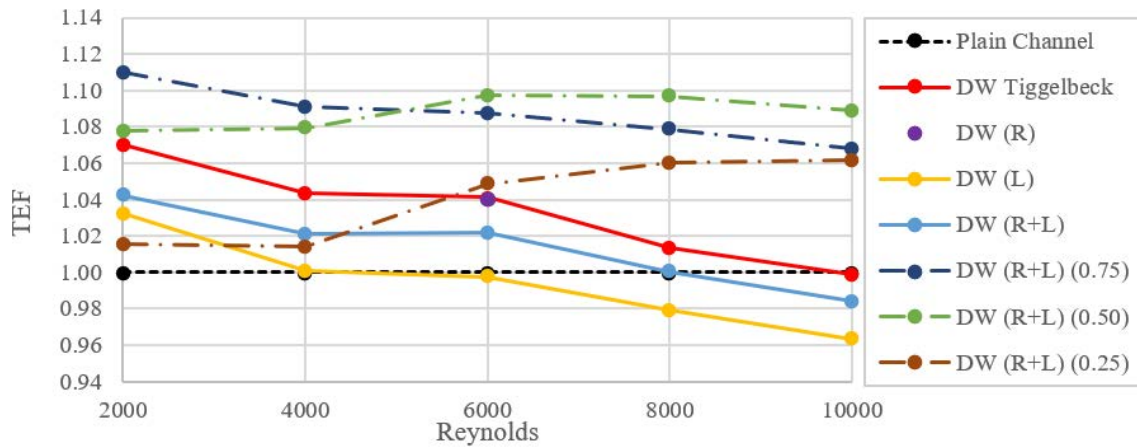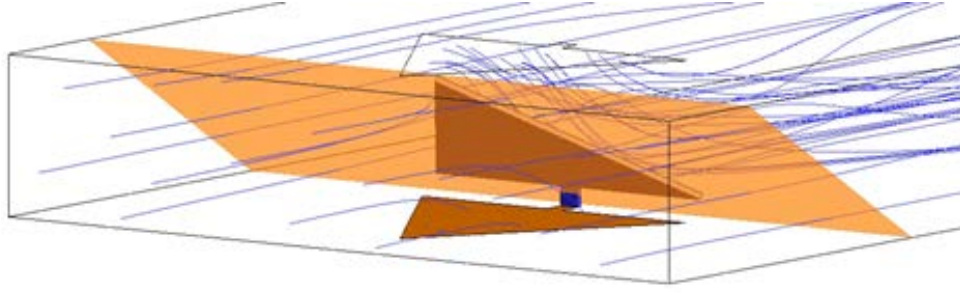**Figure 13.** Hydraulic performance of the study cases

Figure 14. Global performance of the study cases

Table 5. Validation simulation results

Through	DW Tiggelbeck	DW (L)	DW (R)	DW (R+L)
Channel section	88%	90%	91%	92%
Punching hole	12%	10%	9%	8%

Figure 15. Control surfaces for studying flow paths

For DW (R), where the lifting amounted to a surface removal of 20%, an increased flow was directed through the channel section by 3%, yet a significant portion still passed through the punching hole. Consequently, a marginal decrease in system friction was observed, resulting in the highest Nusselt loss and the least effective TEF performance. For DW $(R+L)$, involving a material removal, a slightly better reduction in head loss was achieved, with a minimal impact on Nusselt number and negligible effects on TEF. The case represented a combination of the two previous geometries, with its 5% flow increase in the main channel attributable to both 3% surface removal and 2% lifting, earning a viable operating range extending from 2,000 to just below 8,000.

It has been observed that the lifting effects may be attributed to the restricted flow velocity near the wall, enforced by the no-slip condition at the interface. In contrast, the central region attains free-stream velocity, thereby rendering DW (R) more effective per unit area removed than DW (L). This effectiveness is evidenced by a significant reduction in f, a minimal decrease in Nu, and consequently, enhanced TEF performance. Despite these findings, and considering certain Reynolds number ranges where geometric modifications in channel designs yield improvements over the plain channel, it is noteworthy that none of these mechanisms, individually or collectively, surpassed the performance noted in Tiggelbeck et al.'s study [5]. This discrepancy might be due to the absence of surface removal effects, as claimed by Zhou and Feng [6], or the lack of LVG lift effects, as suggested by Garelli et al. [9]. The latter's model, notably lacking in perforation inclusion, likely impedes alternative flow diversion paths.

In the scope of this study, significant attention was dedicated to investigating the effects of size-ratio modifications on LVGs in air heat exchangers. It was discerned that a reduction in the size of the LVGs markedly influenced the development of the TEF curve. This alteration in size not only vertically shifted the TEF curves but also dramatically altered their trends, resulting in the emergence of distinct regions of optimal performance across varying flow regimes. Concerning the Nusselt number, it was observed, barring discrepancies attributed to model error, that a diminution in the size of the LVG corresponded with a decrease in Nu. Specifically, in the case of DW $(R+L)(0.25)$, the Nu curve exhibited a bi-linear trend. In the laminar-turbulent transition regime (Re = 2,000-4,000), this curve mirrored the behavior of a flat channel, diverging in regions of higher turbulence. Despite a reduction in thermal performance, these size-ratio modifications were found to effectively reduce the friction factor f, thereby enhancing the overall TEF.

Analyzing the impact on TEF, it was established that decreasing LVG dimensions to 75% of the original size caused the TEF curve to ascend vertically while continuing a decreasing trend akin to the initial curve. A reduction to 50% of the original size resulted in an abrupt change in the curve's trajectory, evolving towards a relatively increasing trend. In contrast, a reduction to 25% led to a downward vertical shift in the DW $(R+L)(0.50)$ curve, maintaining a similar upward trajectory as its predecessor.

In operational regimes characterized by $Re = 2,000 - 5,000$, optimal system performance was achieved through a size reduction to 75%, while in regimes with $Re = 5,000 - 10,000$, a 50% size reduction was more efficacious. Despite these modifications enhancing system efficiency across all speeds, further research is required to ascertain the feasibility of achieving flow regime-invariant efficiency. Notably, in the $DW(R + L)(0.50)$ and $DW(R + L)(0.25)$ cases, the improvement in TEF appeared invariant across turbulence transition regimes. Moreover, decreasing the size-ratio from 75% to 50% elicited a transition in the curves from a negative to a positive slope, suggesting the existence of a critical size ratio at which efficiency remains constant. This finding indicates the potential for developing an LVG with a TEF close to 1.09 , independent of the flow regime, thereby ensuring system performance flexibility. However, this hypothesis warrants further empirical validation.

4 Discussion

DW Tiggelbeck remains the most effective design for enhancing heat exchange in the system, though it also induces the most substantial increase in head loss. Nonetheless, its application is advantageous in most flow regimes, achieving a peak TEF of 1.07 at $Re = 2,000$. Geometric modifications such as surface removal and lifting, contrary to expectations, resulted in only a minor reduction in f and a deterioration of Nu. Consequently, these modifications

did not excel beyond the performance of the DW Tiggelbeck design. Conversely, the size-ratio modifications of the geometrically modified vortex generators $DW(R + L)$ profoundly affected their performance. Two alternative configurations were identified, with TEF values ranging from 1.07 to 1.11, surpassing the original design by 3% and 9%. Despite the computational model suggesting an underestimation of TEF results, these modified geometries remained competitive, exceeding the maximum TEF of 1.09 reported by Garelli et al. [9], and surpassing the 6% improvement achieved with skewed winglet pairs by Oneissi et al. [7]. Therefore, incorporating multiple modified LVGs into each plate of a flat plate heat exchanger is projected to elevate its efficiency.

In the realm of concentrating solar thermal energy systems, where sunlight irradiance is focused onto a small surface area, these LVGs could be potentially beneficial. These systems concentrate solar power into a heat exchanger, heating the working fluid to high temperatures. The application of LVGs in such contexts, possibly in tandem with the advancements reported by Agarwal [2] in thermal energy storage systems, could enhance the energy efficiency of these systems. However, the performance of LVGs under the specific properties of these fluids requires prior investigation.

It is pertinent to note that the choice of using the $DW(R + L)$ to study size-ratio effects was arbitrary and warrants investigation in other geometries to generalize its impact. This also applies to the scaling of the global system, which is a crucial aspect to consider in future research endeavors.

5 Conclusions

This study employed numerical simulations in ANSYS Fluent to explore the impact of geometric modifications and size ratio adjustments on delta-wing type vortex generators in air heat exchangers, focusing on Reynolds number regimes from 2,000 to 10,000. The study encompassed a base case of parallel flat plates, an unmodified delta wing case, and six cases with varying modifications.

A thorough mesh convergence analysis was conducted, demonstrating result independence. The computational model's validity was established through comparisons with analytical correlations and replication of an experimental case from the literature, yielding congruent results.

In terms of geometric modifications, it was discerned that surface removal $DW(R)$, insertion lifting $DW(L)$, and their combination $DW(R + L)$ generally detracted from the thermal enhancement of the original delta wing configuration, as documented by Tiggelbeck et al. [5]. In some scenarios, these modifications were even less effective than the base case of a plain channel.

Conversely, size-ratio modifications, particularly the proportional reduction in the size of the geometrically modified $DW(R + L)$, significantly decreased the system's pressure drop while only mildly reducing the Nusselt number. This led to TEF ranging from 1.07 to 1.11, particularly notable between the 75% and 50% final sizes. These modifications substantially surpassed the traditional delta wing design by approximately 3% and 9%. The findings suggest that, irrespective of the insert's shape, adjusting its size can fine-tune its effects and optimize its performance.

To broaden the applicability of these results, future research should investigate the effects of size-ratio on different insertion geometries, the impact of system scaling on size ratio, and the hypothesis of an optimal size-ratio that maintains TEF invariant to the flow regime.

Data Availability

The data used to support the findings of this study are available from the corresponding author upon request.

Conflicts of Interest

The authors declare no conflict of interest.

References

[1] B. I. Master, K. S. Chunangad, A. J. Boxma, D. Kral, and P. Stehlík, "Most frequently used heat exchangers from pioneering research to worldwide applications," *Heat Transf. Eng.*, vol. 27, no. 6, pp. 4–11, 2006. https://doi.org/10.1080/01457630600671960

[2] A. Agarwal, "Heat absorption performance enhancement of TES system using iron oxide/paraffin wax composite," *Power Eng. Eng. Thermophys.*, vol. 2, no. 2, pp. 73–85, 2023. https://doi.org/10.56578/peet020202

[3] P. Deb, G. Biswas, and N. K. Mitra, "Heat transfer and flow structure in laminar and turbulent flows in a rectangular channel with longitudinal vortices," *Int. J. Heat Mass Transf.*, vol. 38, pp. 2427–2444, 1995. https://doi.org/10.1016/0017-9310(94)00357-2

[4] S. Tiggelbeck, N. K. Mitra, and M. Fiebig, "Experimental investigations of heat transfer enhancement and flow losses in a channel with double rows of longitudinal vortex generators," *Int. J. Heat Mass Transf.*, vol. 36, no. 9, pp. 2327–2337, 1993. https://doi.org/10.1016/s0017-9310(05)80117-6

[5] S. Tiggelbeck, N. K. Mitra, and M. Fiebig, "Comparison of wing-type vortex generators for heat transfer enhancement in channel flows," *ASME J. Heat Mass Transf.*, vol. 116, no. 4, pp. 880–885, 1994. https://doi.org/10.1115/1.2911462

[6] G. Zhou and Z. Feng, "Experimental investigations of heat transfer enhancement by plane and curved winglet type vortex generators with punched holes," *Int. J. Therm. Sci.*, vol. 78, pp. 26–35, 2014. https://doi.org/10.1016/j.ijthermalsci.2013.11.010

[7] M. Oneissi, C. Habchi, S. Russeil, D. Bougeard, and T. Lemenand, "Novel design of delta winglet pair vortex generator for heat transfer enhancement," *Int. J. Therm. Sci.*, vol. 109, pp. 1–9, 2016. http://dx.doi.org/10.1016/j.ijthermalsci.2016.05.025

[8] A. T. Wijayanta, I. Yaningsih, M. Aziz, T. Miyazaki, and S. Koyama, "Double-sided delta-wing tape inserts to enhance convective heat transfer and fluid flow characteristics of a double-pipe heat exchanger," *Appl. Therm. Eng.*, vol. 145, pp. 27–37, 2018. https://doi.org/10.1016/j.applthermaleng.2018.09.009

[9] L. Garelli, G. Ríos Rodriguez, J. J. Dorella, and M. A. Storti, "Heat transfer enhancement in panel type radiators using delta-wing vortex generators," *Int. J. ThermSci.*, vol. 137, pp. 64–74, 2019. https://doi.org/10.1016/j.ijthermalsci.2018.10.037

[10] I. Ansys, "Ansys fluent theory guide," *Fluids*, vol. 42, pp. 61–64, 2021.

[11] H. Z. Demirag, M. Dogan, and A. A. Igci, "The numerical analysis of novel type conic vortex generator and comparison with known VGs for heat transfer enhancement," *Heat Mass Transf.*, vol. 58, pp. 735–762, 2022. https://doi.org/10.1007/s00231-021-03117-7

[12] Y. A. Cengel, *Heat Transfer: A Practical Approach.* McGraw-Hill, 2007.

[13] H. K. Tam, L. M. Tam, and A. J. Ghajar, "Effect of inlet geometries and heating on the entrance and fully-developed friction factors in the laminar and transition regions of a horizontal tube," *Exp. Therm. Fluid Sci.*, vol. 44, no. 4, pp. 680–696, 2013. https://doi.org/10.1016/j.expthermflusci.2012.09.008

[14] M. Dogan and A. Abir Igci, "An experimental comparison of delta winglet and novel type vortex generators for heat transfer enhancement in a rectangular channel and flow visualization with stereoscopic PIV," *Int. J. Heat Mass Transf.*, vol. 164, 2021. https://doi.org/10.1016/j.ijheatmasstransfer.2020.120592

[15] G. Haller, "An objective definition of a vortex," *J. Fluid Mech.*, vol. 525, pp. 1–26, 2005. https://doi.org/10.1017/S0022112004002526

Nomenclature

A wall surface, m^2
A_t channel transversal section surface, m^2
b channel breadth, m
C_f LVG breadth, m
C_p specific heat capacity, $\text{J.kg}^{-1} \cdot \text{K}^{-1}$
D_h hydraulic diameter of the channel, m
dx horizontal length of LVG lifting, m
dy vertical length of LVG lifting, m
f skin friction coefficient, dimensionless
F_d channel drag force, N
H channel height, m
$\bar{h}$ mean convective heat transfer, $\text{W} \cdot \text{m}^{-2} \cdot \text{K}^{-1}$
k thermal conductivity, $\text{W} \cdot \text{m}^{-1} \cdot \text{K}^{-1}$
L channel length, m
l original delta-wing height, m
l' geometrically modified wing height, m
LVG longitudinal vortex generator
m horizontal length of surface removal, m
n vertical length of surface removal, m
n' modified LVG vertical length of removal, m
Nu mean Nusselt number, dimensionless
p total pressure, Pa
p_{dyn} dynamic pressure, Pa
p_{st} static pressure, Pa
Pr Prandtl number, dimensionless
P_W wet perimeter of transversal section, m
Q Q-criterion, s^{-2}
$\dot{Q}$ convective heat transfer rate, W
Re Reynolds number, dimensionless
T temperature, K
T_{in} inlet mean bulk temperature, K
T_m mean temperature between inlet and wall, K
T_{out} outlet mean bulk temperature, K
T_W wall temperature, K K
TEF thermal enhancement factor, dimensionless
u fluid speed at inlet, m.s^{-1}

Greek symbols

ρ density, $\text{kg} \cdot \text{m}^{-3}$
μ dynamic viscosity, $\text{kg} \cdot \text{m}^{-1} \cdot \text{s}^{-1}$
β angle of attack, °

Subscripts

in inlet
out outlet
m mean
0 base case